HHS Public Access

Author manuscript

IEEE Antennas Wirel Propag Lett. Author manuscript; available in PMC 2017 June 08.

Published in final edited form as:

IEEE Antennas Wirel Propag Lett. 2016 May 3; 16: 1431–1434. doi:10.1109/LAWP.2016.2561903.

Modeling and Measurement of Radio Propagation in Tunnel Environments

Chenming Zhou [Member, IEEE] and

National Institute for Occupational Safety and Health/Centers for Disease Control and Prevention (NIOSH/CDC), Pittsburgh, PA 15236 USA

Ronald Jacksha

National Institute for Occupational Safety and Health, Pittsburgh, PA 15236 USA

Abstract

A simple radio frequency (RF) testing system that can be conveniently built and used for measuring radio propagation in tunnels is introduced. With the proposed testing system, RF power attenuation with distance in a train tunnel was measured at four frequencies (455, 915, 2450, and 5800 MHz) for both horizontal and vertical polarizations. Two analytical modeling methods—the ray tracing and modal methods—are applied to model RF propagation in the tunnel. The theoretical predictions based on both methods are compared to field measurements and find good agreement.

Index Terms

Modal method; ray tracing; tunnel propagation

I. Introduction

IN THE event of an underground emergency, it is critical for underground miners to communicate with and be tracked by personnel on the surface. As mandated by the 2006 Mine Improvement and New Emergency Response Act (MINER Act) [1], communication and tracking devices are now required in all US underground coal mines. The performance of installed systems is highly dependent on the underground wireless channel. Coal mines generally consist of a series of parallel and perpendicular tunnels referred to respectively as entries and crosscuts. The propagation characteristics in these confined entries and crosscuts are similar to those in road tunnels, where radio frequency (RF) propagation characteristics have been extensively investigated [2].

Two analytical methods, namely the ray tracing [3] and modal methods [4], [5], have been applied to model the wireless channels in tunnel environments. The ray tracing method

Color versions of one or more of the figures in this letter are available online at http://ieeexplore.ieee.org.

Digital Object Identifier 10.1109/LAWP.2016.2561903

Disclaimer: The findings and conclusions in this paper are those of the authors and do not necessarily represent the views of the National Institute for Occupational Safety and Health.

views radio waves as ray tubes that can be reflected by four surfaces of the tunnel. The received power is obtained by summing up the contributions of the rays that reach the receiver. The modal method, on the other hand, treats radio waves in a tunnel as modes in a waveguide, and the received power is obtained by summing up the contributions of modes. The two methods have been treated as two completely different methods in the past, and researchers generally use one of them for modeling radio propagation in tunnels. Recently, the two methods were shown to be mathematically equivalent [6].

In this letter, we validate the ray tracing and modeling methods with extensive measurements performed in a train tunnel. Theoretical predictions based on the two analytical methods are compared to the measurement results taken at different frequencies and polarizations and show good agreement. In addition, we propose a new RF measurement system that can be conveniently used for measuring radio propagation in tunnels. Compared to vector-network-analyzer-based testing systems that were commonly reported in the literature for measuring tunnel propagation, the proposed system is relatively simpler and easier to setup and use.

II. Modeling Methods

We consider a straight rectangular tunnel with four flat surfaces. Let $\bar{\varepsilon}_{a,b}=[\varepsilon_{a,b}-j\sigma_{a,b}/(2\pi f)]/\varepsilon_0$ denote the complex relative permittivities of the vertical and horizontal walls, respectively. Here, f is the frequency, and $\varepsilon_{a,b}$ and $\sigma_{a,b}$ are the permittivities and conductivities of the corresponding tunnel walls. The width and height of the tunnel are $2a$ and 2b, respectively. Within the tunnel, a transmitter is located at $T(x_0, y_0, 0)$ and a receiver at $R(x, y, z)$. Without loss of generality, we also assume the source is vertically polarized.

A. Ray Tracing Method

Based on the ray tracing theory, the received electric field in a tunnel can be calculated as [7]

$$E_{\mathrm{r}}(x,y,z)=E_{\mathrm{t}}\sum_{m=-\infty}^{+\infty}\sum_{n=-\infty}^{+\infty}\frac{e^{-jkr_{m,n}}}{r_{m,n}}\rho_{\perp}^{|m|}\rho_{//}^{|n|} \quad (1)$$

where E_{t} is the magnitude of the transmitted electric field and k is the wavenumber in the waveguide (free space). The other parameters in (1) are given by

$$r_{m,n}=\sqrt{(2ma+(-1)^m x_0-x)^2+(2nb+(-1)^n y_0-y)^2+z^2} \quad (2)$$

$$\rho_{\perp}=\frac{\cos\theta_{\perp}-\sqrt{\bar{\varepsilon}_a-1+\cos^2\theta_{\perp}}}{\cos\theta_{\perp}+\sqrt{\bar{\varepsilon}_a-1+\cos^2\theta_{\perp}}}$$
$$\rho_{//}=\frac{\cos\theta_{//}-\sqrt{\bar{\varepsilon}_b-1+\cos^2\theta_{//}}/\bar{\varepsilon}_b}{\cos\theta_{//}+\sqrt{\bar{\varepsilon}_b-1+\cos^2\theta_{//}}/\bar{\varepsilon}_b} \quad (3)$$

$$\begin{aligned} cos\theta_{\perp} &= \frac{|2ma+(-1)^m x_0 - x|}{r_{m,n}} \\ cos\theta_{//} &= \frac{|2nb+(-1)^n y_0 - y|}{r_{m,n}}. \end{aligned} \quad (4)$$

It should be noted that only reflections are considered in the above ray tracing model and diffractions have been ignored. For straight tunnels with smooth walls, this assumption is generally valid [7].

B. Modal Method

As shown in [6], the electric field at an arbitrary position within a dielectric rectangular tunnel can also be viewed as the superposition of the electric fields from different hybrid modes ($EH_{p,q}$)

$$E_r = \frac{-j2\pi E_t}{ab} \sum_{p=1}^{+\infty} \sum_{q=1}^{+\infty} A_{p,q} \frac{e^{-(\alpha_{p,q}+j\beta_{p,q})z}}{\beta_{p,q}} \quad (5)$$

where

$$\begin{aligned} A_{p,q} = & sin\ \left(\frac{p\pi}{2a}x + \varphi_p\right)\ sin\ \left(\frac{q\pi}{2b}y + \varphi_q\right) \\ & \times sin\ \left(\frac{p\pi}{2a}x_0 + \varphi_p\right)\ sin\ \left(\frac{q\pi}{2b}y_0 + \varphi_q\right) \end{aligned} \quad (6)$$

$$\varphi_{p,q} = \begin{cases} 0, & p\,(q)\ \text{is even} \\ \pi/2, & p\,(q)\ \text{is odd} \end{cases} \quad (7)$$

$$\beta_{p,q} = \sqrt{k^2 - \left(\frac{p\pi}{2a}\right)^2 - \left(\frac{q\pi}{2b}\right)^2} \quad (8)$$

$$\alpha_{p,q} = \frac{1}{b}\left(\frac{q\lambda}{4b}\right)^2 \frac{\bar{\varepsilon}_b}{\sqrt{\bar{\varepsilon}_b - 1}} + \frac{1}{a}\left(\frac{p\lambda}{4a}\right)^2 \frac{1}{\sqrt{\bar{\varepsilon}_a - 1}}. \quad (9)$$

III. Measurement Methods

Measurements were taken in an out-of-service railroad tunnel with its cross-sectional view shown in Fig. 1(a). The tunnel is rectangular with an arched roof. The height of the tunnel is 6.7 m, and the width of the tunnel is 4.9 m. The length of the tunnel is about 800 m. The walls and ceiling are fairly smooth with some rough sections due to deterioration of the concrete. The rails and ties have been removed, leaving only the crushed stone track ballast.

The tunnel is straight and has no noticeable slope. Both the transmitter and receiver antennas were set to a height of 2.14 m and placed in the center between the left and right walls of the tunnel. The associated modeling and measurement results with antennas placed at off-center locations were reported in [8].

A simple RF testing system was devised for measuring radio propagation. The RF test apparatus was comprised of two components: a stationary RF transmitter and a mobile RF receiver [shown in Fig. 1(b)]. The transmitter (Tx) consisted of an AnaPico Aspin 6000 RF signal source connected to one of four frequency-specific collinear J-pole antennas; a Laird FG4500, Laird FG8960, Laird FG24005, or a SuperPass SPDJ40. The receiver (Rx) consisted of a Tektronix H600RF spectrum analyzer connected through an RF A/B switch to either a 50-Ω termination or one of the four antennas. Receiver mobility was accomplished by means of a backpack frame assembly, which mounted the spectrum analyzer in front of the wearer with the Rx antenna located above and slightly to the rear of the wearer. RF signal propagation was measured as follows: The RF signal source was configured to produce a continuous wave signal with a fixed output power of 3 dBm that was verified at the Tx antenna using an RF power meter. The spectrum analyzer's input was switched to the Rx antenna, and the wearer of the backpack assembly walked away from, or back toward, the transmitter. At presurveyed intervals of distance—typically 30 m—travel was halted and the spectrum analyzer's input was momentarily switched to the 50-Ω termination. This inserted a received power null into the measured data, which served as a distance indicator. The spectrum analyzer's input was then switched back to the Rx antenna and travel was resumed. Postprocessing of the logged data was performed to correlate the inserted power nulls in the data to the presurveyed distances. It is assumed that there is no significant speed variation between the two adjacent power nulls (distance calibration points). In addition, during the measurements, an antenna polarization switch is done by rotating the antenna from a vertical mounting to a horizontal mounting or vice versa.

IV. Numerical and Measurement Results

Fig. 2 shows an example of the raw measurement data with nulls generated by manually switching the input of the spectrum analyzer to the 50-Ω termination. The horizontal axis is the index of the logged data points, which is directly related to the timestamp of the logged data. The postprocessed results for Fig. 2 with nulls removed are shown in Fig. 3, where the horizontal axis becomes the separation distance between the transmitter and the receiver. Fig. 3 also shows two other plotted measurement results used for cross-verification purposes. Three different methods were used to measure the tunnel propagation loss in Fig. 3. In the first method "MovingRx:Fwd," the received power is measured while the receiver is traveling away from a stationary transmitter. For the second method "MovingRx:Rev," the receiver starts at the other end of the tunnel and moves toward the stationary transmitter. To verify the channel reciprocity, in the third method, labeled "MovingTx:Fwd," we switch the position of the transmitter and receiver so the receiver is stationary and transmitter is mobile.

It is shown in Fig. 3 that the power measurements using all three methods are consistent with each other, indicating that the wireless channel in the tunnel is reciprocal and independent of travel direction. This good agreement also confirms that the measurement result is very

repeatable, in which the “MovingTx:Fwd” measurement was actually performed 50 days after the other two measurements in Fig. 3.

Figs. 4–6 show a comparison between the simulated and the measured power distributions within the tunnel for different frequencies and polarizations. The ray tracing simulation results (shown as a dashed-dotted line) are generated based on (1), while the mode results (shown as a dashed line) are based on (5). It should be noted that both the ray tracing and modal methods presented in the letter are derived based on rectangular tunnels. The cross section of the tunnel where the measurements were carried out is not an “exact” rectangle as the ceiling of the tunnel is arched. In order to apply the two methods to model radio propagation in the measurement tunnel, we have approximated the cross section of the measurement tunnel by an equivalent rectangle with the same width of 4.9 m and a height of 6.6 m. The height of the approximated equivalent rectangle is determined by best fitting the simulation data to the measurement data. In addition, the same electrical properties ($Re\{\bar{\varepsilon}_{a,b}\}=7$ and $\sigma_{a,b}$= 0.05 S/m) are used for all four tunnel walls and all four frequencies. It is shown from Figs. 4–6 that the ray and modal methods yield the same results, which also agree reasonably well with the measured results. The discrepancies between the measured and simulated results in Fig. 6 for high-frequency signals can be explained by the fact that both the ray tracing and modal are less accurate for modeling short-term rapid power fluctuations caused by the interaction of many modes. For low-frequency signals, higher order modes decay much faster with distance, so the two modeling methods show better accuracy as observed in Figs. 4 and 5.

As shown in (1) and (5), theoretically, an infinite number of rays (or modes) should be included in the model to accurately calculate the received signal. Practically, however, only a limited number of rays/modes will be considered. For the results reported in this letter, the maximum order of the images and modes used in (1) and (5) has been limited to a fixed number of 80, which has been tested to be sufficient for all the distances.

V. Conclusion

A simple RF testing system that can be conveniently used for measuring radio propagation in tunnels was proposed. We show that the proposed system can give reliable and repeatable measurement results. With the proposed system, propagation measurements at four different frequencies and for both the vertical and horizontal polarizations were taken in an out-ofservice railroad tunnel. Ray tracing and modal methods were applied to model radio propagation in the tunnel. The modeling results show very good agreement with the measured results for different frequencies and polarizations. Based on the results, major propagation controlling factors including frequency, tunnel dimensions, polarization, and wall electrical properties can be identified. Those controlling factors should be considered in the design and deployment of optimum communication systems in underground mines. For example, it is suggested that antenna polarization should be chosen based on the dimension ratio of the tunnel. For tunnels where the height is greater than the width such as the one shown in this letter, vertical polarization should be used for a better signal coverage.

Acknowledgments

The authors would like to thank T. Plass for his help on taking the measurement data. They would also like to thank Dr. J. Waynert for many useful discussions.

References

1. United States Public Laws, Mine Improvement and New Emergency Response Act of 2006 (MINER Act). PL 109–236. 2006.
2. Dudley DG, Lienard M, Mahmoud SF, Degauque P. Wireless propagation in tunnels. IEEE Antennas Propag Mag. Apr.2007 49(2):11–26.
3. Mahmoud SF, Wait JR. Geometrical optical approach for electromagnetic wave propagation in rectangular mine tunnels. Radio Sci. 1974; 9:1147–1158.
4. Laakmann KD, Steier WH. Waveguides: Characteristic models of hollow rectangular dielectric waveguides. Appl Opt. May.1976 15:1334–1340. [PubMed: 20165176]
5. Emslie A, Lagace R, Strong P. Theory of the propagation of UHF radio waves in coal mine tunnels. IEEE Trans Antennas Propag. Mar.1975 AP-23(2):192–205.
6. Zhou C, Waynert J. The equivalence of the ray tracing and modal methods for modeling radio propagation in lossy rectangular tunnels. IEEE Antennas Wireless Propag Lett. 2014; 13:615–618.
7. Zhou C, Waynert J, Plass T, Jacksha R. Attenuation constants of radio waves in lossy-walled rectangular waveguides. Prog Electromagn Res. 2013; 142:75–105.
8. Zhou, C., Jacksha, R. Modeling and measurement of the influence of antenna transversal location on tunnel propagation. Proc IEEE Int Symp Antennas Propag; Vancouver, BC, Canada. Jul. 2015; p. 81-82.

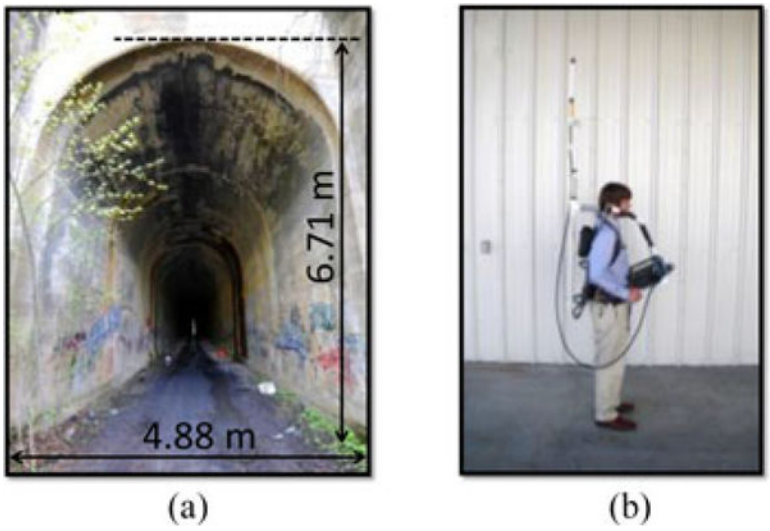

Fig. 1.

(a) Entrance of the tunnel and (b) the mounted receiver used for the propagation measurements in the tunnel.

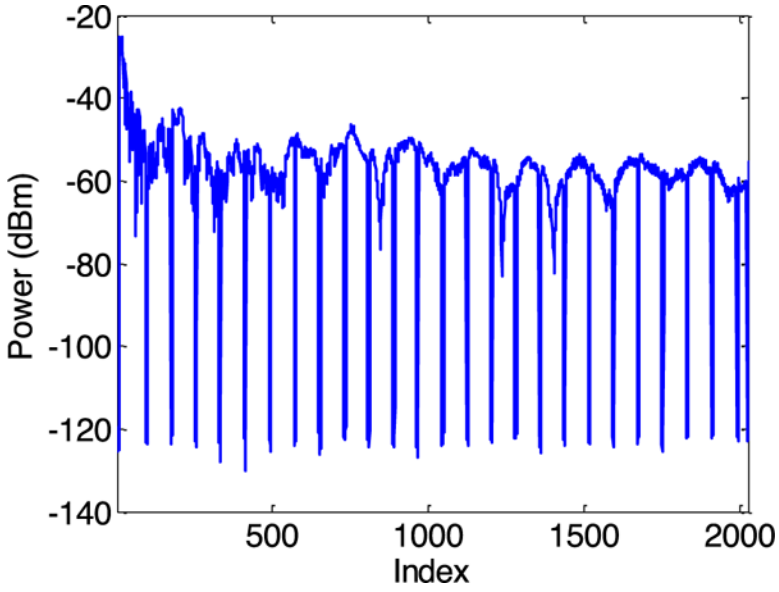

Fig. 2.
Example of the raw measurement data with nulls that serve as distance indicators.

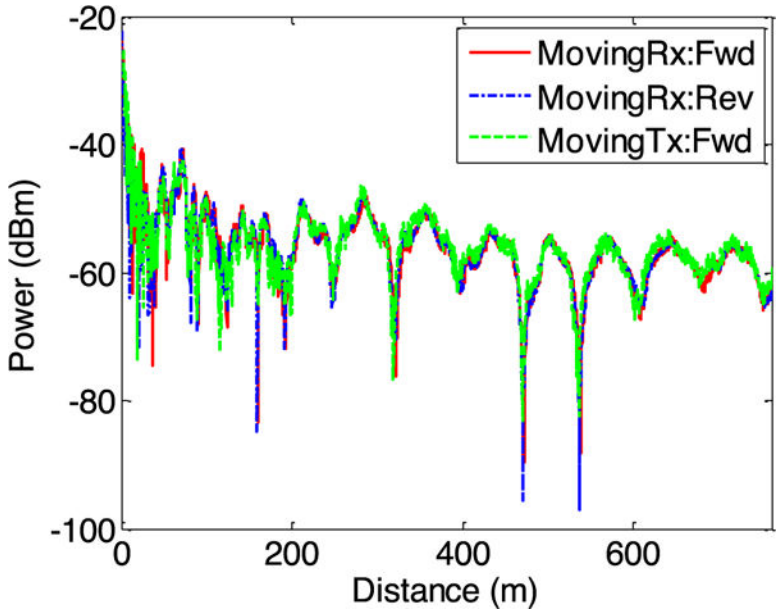

Fig. 3.

Measurement results for channel reciprocity and moving direction tests (915 MHz, vertical polarization).

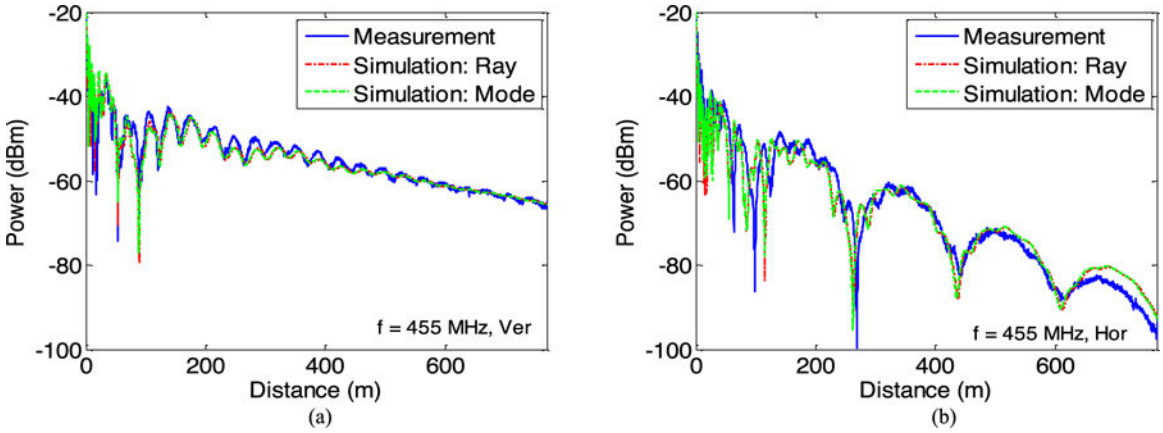

Fig. 4.

Simulation and measurement results comparison at f = 455 MHz. (a) Vertical. (b) Horizontal.

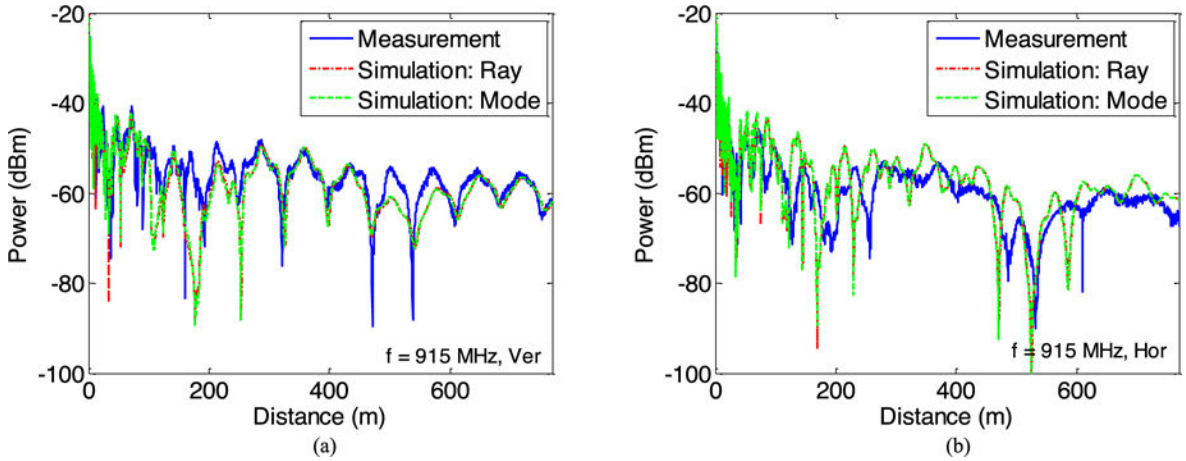

Fig. 5.

Simulation and measurement results comparison at f = 915 MHz. (a) Vertical polarization. (b) Horizontal polarization.

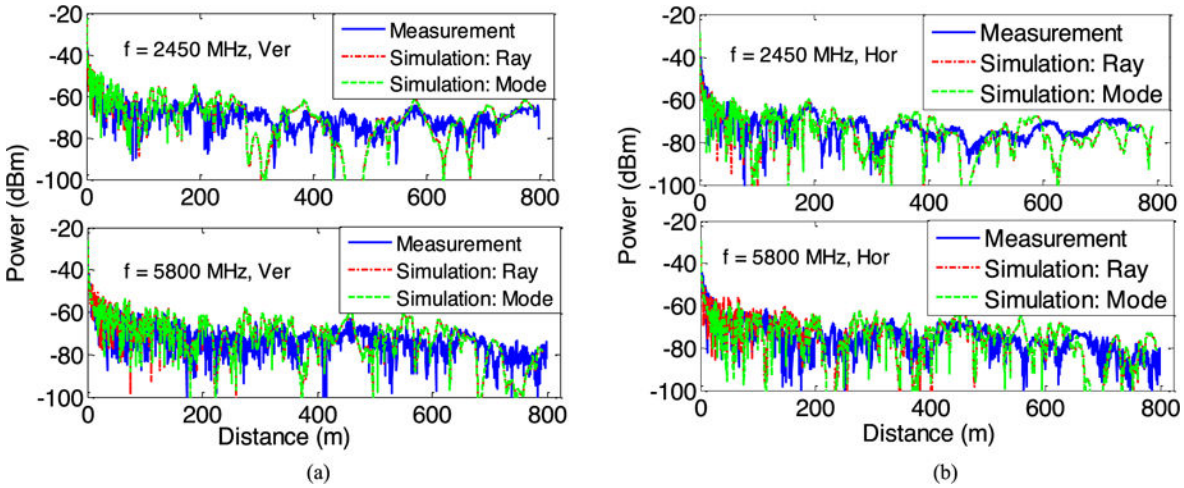

Fig. 6.

Simulation and measurement results comparison at f = 2450 MHz and 5800 MHz signals. (a) Vertical polarization. (b) Horizontal polarization.